

Dissecting the region around IceCube-170922A: the blazar TXS 0506+056 as the first cosmic neutrino source

P. Padovani¹, P. Giommi^{2,3,4}, E. Resconi⁵, T. Glauch⁵, B. Arsoli^{6,7}, N. Sahakyan⁸, M. Huber⁵

¹European Southern Observatory, Karl-Schwarzschild-Str. 2, D-85748 Garching bei München, Germany

²Agenzia Spaziale Italiana, ASI, via del Politecnico s.n.c., I-00133 Roma Italy

³Institute for Advanced Studies, Technische Universität München, Lichtenbergstrasse 2a, D-85748 Garching bei München, Germany

⁴ICRANet, Piazzale della Repubblica, 10 - 65122, Pescara, Italy

⁵Technische Universität München, Physik-Department, James-Frank-Str. 1, D-85748 Garching bei München, Germany

⁶Instituto de Física Gleb Wataghin, UNICAMP, R. Sérgio Buarque de Holanda 777, 13083-859 Campinas, Brazil

⁷ICRANet-Rio, CBPF, Rua Dr. Xavier Sigaud 150, 22290-180 URCA, Rio de Janeiro, Brazil

⁸ICRANet-Armenia, Marshall Baghramian Avenue 24a, 0019 Yerevan, Republic of Armenia

Accepted XXX. Received YYY; in original form ZZZ

ABSTRACT

We present the dissection in space, time, and energy of the region around the IceCube-170922A neutrino alert. This study is motivated by: (1) the first association between a neutrino alert and a blazar in a flaring state, TXS 0506+056; (2) the evidence of a neutrino flaring activity during 2014–2015 from the same direction; (3) the lack of an accompanying simultaneous γ -ray enhancement from the same counterpart; (4) the contrasting flaring activity of a neighbouring bright γ -ray source, the blazar PKS 0502+049, during 2014–2015. Our study makes use of multi-wavelength archival data accessed through Open Universe tools and includes a new analysis of *Fermi*-LAT data. We find that PKS 0502+049 contaminates the γ -ray emission region at low energies but TXS 0506+056 dominates the sky above a few GeV. TXS 0506+056, which is a very strong (top percent) radio and γ -ray source, is in a high γ -ray state during the neutrino alert but in a low though hard γ -ray state in coincidence with the neutrino flare. Both states can be reconciled with the energy associated with the neutrino emission and, in particular during the low/hard state, there is evidence that TXS 0506+056 has undergone a hadronic flare with very important implications for blazar modelling. All multi-messenger diagnostics reported here support a single coherent picture in which TXS 0506+056, a very high energy γ -ray blazar, is the only counterpart of all the neutrino emissions in the region and therefore the most plausible first non-stellar neutrino and, hence, cosmic ray source.

Key words: neutrinos — radiation mechanisms: non-thermal — galaxies: active — BL Lacertae objects: general — gamma-rays: galaxies

1 INTRODUCTION

The IceCube Neutrino Observatory at the South Pole¹ has recently reported the detection of a number of high-energy astrophysical neutrinos² (Aartsen et al. 2013; IceCube Collaboration 2013, 2014, 2015a). These include 82 high-energy starting events collected over six years (IceCube Collaboration 2017b), which are inconsistent with a purely atmospheric origin with a significance greater than 6.5σ . The Ice-

Cube signal, including the 34 through-going charged current ν_μ from the northern sky (Aartsen et al. 2015; IceCube Collaboration 2015b; Aartsen et al. 2016; IceCube Collaboration 2017a), is still compatible with an isotropic distribution. The origin of the IceCube neutrinos is presently unknown (see, e.g. Ahlers & Halzen 2015, and references therein, for a comprehensive discussion) although various hints consistently point to blazars as one of the most probable candidates, as described below.

The Large Area Telescope (LAT) on-board the *Fermi* Gamma-ray Space Telescope is a pair-conversion telescope sensitive to high energy photons with energies from 20 MeV

¹ <http://icecube.wisc.edu>

² In this paper neutrino means both neutrino and anti-neutrino.

to greater than 300 GeV (Atwood et al. 2009) that has been surveying the γ -ray sky for the past almost 10 years. The constant monitoring and archiving of all-sky γ -ray data permits unprecedented investigations of variable sources.

To explore the complexity of the multi-wavelength sky, we make use of innovative tools that are under development within “Open Universe”, a new initiative under the auspices of the United Nations Committee On the Peaceful Uses of Outer Space (COPUOS). The goal of Open Universe is to stimulate a large increase of the accessibility and usability of space science data in all sectors of society from the professional scientific community, to universities, schools, museums, and citizens. A web portal of the Open Universe initiative, developed at the Italian Space Agency, is available at openuniverse.asi.it. In this paper we make use of software, such as the VOU-BLAZAR tool, which has been specifically designed to identify blazars based on multi-frequency information in large error regions, and spectral energy distribution (SED) animations.

Blazars are active galactic nuclei (AGN; see Padovani et al. 2017, for a recent AGN review) having a relativistic jet that is seen at a small angle with respect to the line of sight. The jet contains charged particles moving in a magnetic field emitting non-thermal radiation over the entire electromagnetic spectrum (Urry & Padovani 1995; Padovani et al. 2017). Since the energy distribution of these particles can significantly differ from object to object, the electromagnetic emission exhibits a wide range of intensity levels and spectral slopes across the spectrum. This results in observational properties that depend strongly on the energy band where blazars are discovered. In a series of papers Giommi et al. (2012a, 2013); Padovani & Giommi (2015); Giommi & Padovani (2015) proposed a new blazar paradigm (but see Ghisellini et al. 2017, for an alternative scenario) based on dilution by the jet and the host galaxy, minimal assumptions on the physical properties of the non-thermal jet emission, and unified schemes. By means of detailed Monte Carlo simulations, it was shown that this scenario is consistent with the complex observational properties of blazars as we know them in all parts of the electromagnetic spectrum.

The possibility that blazars could be the sources of high-energy neutrinos has been investigated by many authors, even long before the IceCube detections (e.g. Mannheim 1995; Halzen & Zas 1997; Mücke et al. 2003; Padovani & Resconi 2014; Petropoulou et al. 2015; Tavecchio & Ghisellini 2015).

Padovani et al. (2016) have correlated the second catalogue of hard *Fermi*-LAT sources (2FHL, $E > 50$ GeV, Ackermann et al. 2016) and other catalogues, with the publicly available high-energy neutrino sample detected by IceCube. The chance probability of association of 2FHL high-energy peaked blazars (HBL/HSP, i.e. sources with the peak of the synchrotron emission $\nu_{\text{peak}}^S > 10^{15}$ Hz³; Padovani & Giommi 1995) with IceCube events was 0.4 per cent, which becomes 1.4 per cent (2.2σ) by evaluating the impact of trials (Resconi et al. 2017). This hint appears to be strongly dependent on γ -ray flux. The corresponding fraction of the

IceCube signal explained by HBL is however only $\sim 10 - 20$ per cent, which agrees with the results of Aartsen et al. (2017); IceCube Collaboration (2017c), who by searching for cumulative neutrino emission from blazars in the second *Fermi*-LAT AGN (2LAC; Ackermann et al. 2011) and other catalogues (including also the 2FHL), have constrained the maximum contribution of known blazars to the observed astrophysical neutrino flux to < 27 per cent.

High-energy astrophysical neutrinos originate in cosmic ray interactions providing a natural link with high-energy and possibly ultrahigh-energy cosmic ray (UHECR) detection. Resconi et al. (2017) have presented a hint of a connection between HBL, IceCube neutrinos, and UHECRs ($E \geq 52 \times 10^{18}$ eV) with a probability ~ 0.18 per cent (2.9σ) after compensation for all the considered trials. Even in this case, HBL can account only for ≈ 10 per cent of the UHECR signal.

None of the possible neutrino counterparts in Padovani et al. (2016) and Resconi et al. (2017) are tracks, as they are all cascade-like events⁴. This indicates that by using tracks we are still limited in sensitivity to the HBL neutrino signal. Although tracks trace only about 1/6 of the astrophysical signal for a flavour ratio $\nu_e : \nu_\mu : \nu_\tau = 1 : 1 : 1$, standard neutrino cross-sections, and IceCube event selection efficiencies, after a long enough exposure a track IceCube signal from blazars should also start to appear. This is of great interest, because false (random) associations of tracks with a blazar are unlikely due to the better defined position of this event-class with respect to cascades.

Recently Lucarelli et al. (2017a) have found a transient γ -ray (> 100 MeV) *AGILE* source positionally coincident with an IceCube track with a post-trial significance $\sim 4\sigma$ and possibly associated with an HBL. However, no other space missions nor ground observatories have reported any detection of transient emission consistent with this event.

The most probable hint of an association ($3 - 3.5\sigma$) reported so far (IceCube Collaboration 2018a) between an IceCube astrophysical neutrino and an extragalactic object is that of the neutrino IceCube-170922A and the radio bright (~ 1 Jy at 5 GHz) and γ -ray flaring BL Lac object TXS 0506+056 (also known as 5BZB J0509+0541, 2FHL J0509.5+0541, and 3FGL J0509.4+0541). Moreover, IceCube has reported in IceCube Collaboration (2018b) an independently observed 3.5σ excess of neutrinos from the direction of TXS 0506+056 between October 2014 and February 2015 providing further indication of a high-energy neutrino association.

The presence of several non-thermal objects including variable blazars within 80 arc-minutes of IceCube-170922A (that is within the size of the *Fermi*-LAT point spread function [PSF⁵], which is $\sim 2.8^\circ$ [95 per cent containment] at $E = 1$ GeV) makes the γ -ray emission from this area quite complex, with possible source confusion. Different objects

³ Blazars can be further divided into low (LBL: $\nu_{\text{peak}}^S < 10^{14}$ Hz) and intermediate (IBL: 10^{14} Hz $< \nu_{\text{peak}}^S < 10^{15}$ Hz) energy peaked sources.

⁴ The topology of IceCube detections can be broadly classified in two types: (1) cascade-like, characterized by a compact spherical energy deposition, which can only be reconstructed with a spatial resolution $\approx 15^\circ$; (2) track-like, defined by a dominant linear topology from the induced muon, with positions known typically within one degree or less.

⁵ The Fermi PSF for this analysis event selection has been determined using the *gtps* Fermi Science Support Center tool.

could in fact contribute to the overall γ -ray flux at different levels in a time-dependent manner. For this reason, we report here on what we have called the *dissection* of the region around IceCube-170922A taking into account the fact that all sources present in the area could be in principle contributors to the neutrino emission observed in 2014–2015 and in 2017. We use innovative software tools that exploit all the publicly available multi-frequency data to study in detail the area around the position of IceCube-170922A at all energies and in the time domain, together with a very careful analysis of the γ -ray emission, providing a wide perspective in space and time.

Section 2 describes the multi-messenger data we used, while Section 3 puts them all together to study the relevant sources in the area, their γ -ray light curves and SEDs. Section 4 gives our results, which are discussed in Section 5. Section 6 summarizes our conclusions. We use a Λ CDM cosmology with Hubble constant $H_0 = 70 \text{ km s}^{-1} \text{ Mpc}^{-1}$, matter density $\Omega_{m,0} = 0.3$, and dark energy density $\Omega_{\Lambda,0} = 0.7$.

2 MULTI-MESSENGER DATA ANALYSIS

2.1 Neutrino data

2.1.1 The IceCube-170922A alert event

The high-energy upward-going muon IceCube-170922A reported by IceCube through a Gamma-ray Coordinates Network Circular on MJD 58018 (September 22, 2017; [Kopper & Blaufuss 2017](#)) originates from a neutrino with $E_\nu \sim 290 \text{ TeV}$, which is probably of astrophysical origin. The best-fit reconstructed position is right ascension (RA) $77.43^{+0.95}_{-0.65}$ and declination (Dec) $+5.72^{+0.50}_{-0.30}$ (deg, J2000, 90 per cent containment region: [IceCube Collaboration 2018a](#)). No other high-energy neutrino passing the same selection of alert-like events has been observed from this direction from 2010 onwards until today.

[IceCube Collaboration \(2018a\)](#) have derived the coincidence probability as a measure of the likelihood that a neutrino alert like IceCube-170922A is correlated by chance with a flaring blazar, considering the large number of known γ -ray sources and the modest number of neutrino alerts. This has been done through several hypothesis tests covering a range of assumptions on the spatial and temporal signal distribution and neutrino emission scenarios. The derived probability was trial-corrected by multiplying the p-value by 51, which correspond to the number of alerts issued by IceCube (10) plus the 41 inspected archival events, which would have triggered alerts if the realtime system had been operational. The final post-trial coincidence probability ranges between 2.5×10^{-4} and 1.3×10^{-3} ($3 - 3.5 \sigma$).

2.1.2 The IceCube neutrino flare in 2014–2015

In contrast with the neutrino alert discussed above, which is a single event identified in real time and satisfying stringent selection criteria, we define here a neutrino flare as a statistically significant ($> 3 \sigma$) accumulation of neutrinos coming from a specific direction over a well-defined time period.

As reported in [IceCube Collaboration \(2018b\)](#), the investigation of the historical 9.5 years of IceCube data at the

position of TXS 0506+056 revealed an excess with a post-trial coincidence probability 2×10^{-4} (3.5σ) over 110^{+35}_{-24} days corresponding to a ν_μ fluence at 100 TeV of $2.1^{+0.9}_{-0.7} \times 10^{-4} \text{ TeV cm}^{-2}$, spectral index $\gamma = 2.1 \pm 0.2$, and an energy range (68 per cent) between 32 TeV and 3.6 PeV ($3.6 \times 10^{15} \text{ eV}$)⁶. This could be interpreted as the first evidence of high-energy neutrino emission from the direction of a known source and comes from an excess of ~ 13 neutrino events between MJD 56949 and 57059 (October 19, 2014 – February 6, 2015).

2.2 Radio and optical monitoring data

The radio (15 GHz) and optical (V_{mag}) data have been taken from the Owens Valley Radio Observatory (OVRO⁷) database, the Catalina Real time Transient Survey (CRTS⁸) and from the All Sky Automatic Survey (ASAS⁹; [Kochanek et al. 2017](#)) online services.

2.3 X-ray and optical/UV data

The *Neil Gehrels Swift* observatory ([Geherls et al. 2004](#)) carried out a total of 92 observations within 80 arc-minutes of IceCube-170922A. Of these, 35 were performed before the arrival of the neutrino and were mostly pointed at the nearby flat spectrum radio quasar (FSRQ) PKS 0502+049. The remaining pointings have been carried out either as a Target of Opportunity follow up mapping the error region of IceCube-170922A a few hours after the event ([Keivani et al. 2017](#)), or as part of the monitoring program of the blazar TXS 0506+056 triggered by the IceCube neutrino alert.

We have analyzed all 92 X-Ray Telescope (XRT; [Burrows et al. 2005](#)) observations using the latest version of the *Swift* data reduction software (HEADAS 6.22) applying standard procedures. This led to the detection of 251 X-ray sources, which were combined with those of existing X-ray catalogues to build Fig. 1 (left). X-ray spectral data were used together with the available multi-frequency data to assemble the SEDs of all interesting sources in the field (see Sect. 3.1).

All optical and UV data of the *Swift* Ultra-Violet and Optical telescope (UVOT; [Romling et al. 2005](#)) for TXS 0506+056 and PKS 0502+049 were analyzed using the SSDC online interactive archive¹⁰.

The *NuSTAR* hard X-ray observatory ([Harrison et al. 2013](#)) was pointed twice, on September 29 and October 19 2017, at TXS 0506+056 following the detection of IceCube-170922A. A few days after the observations the data were made openly available. We have analyzed these data sets using the online analysis tool of the SSDC archives following the standard procedure. In both observations the spectral shape shows a sharp hardening at about 4–5 keV.

⁶ We use here the results obtained for the Gaussian time window because they are the most significant.

⁷ <http://www.astro.caltech.edu/ovroblazars/>

⁸ <http://crts.caltech.edu>

⁹ <http://www.astrouw.edu.pl/asas/>

¹⁰ <http://www.asdc.asi.it>

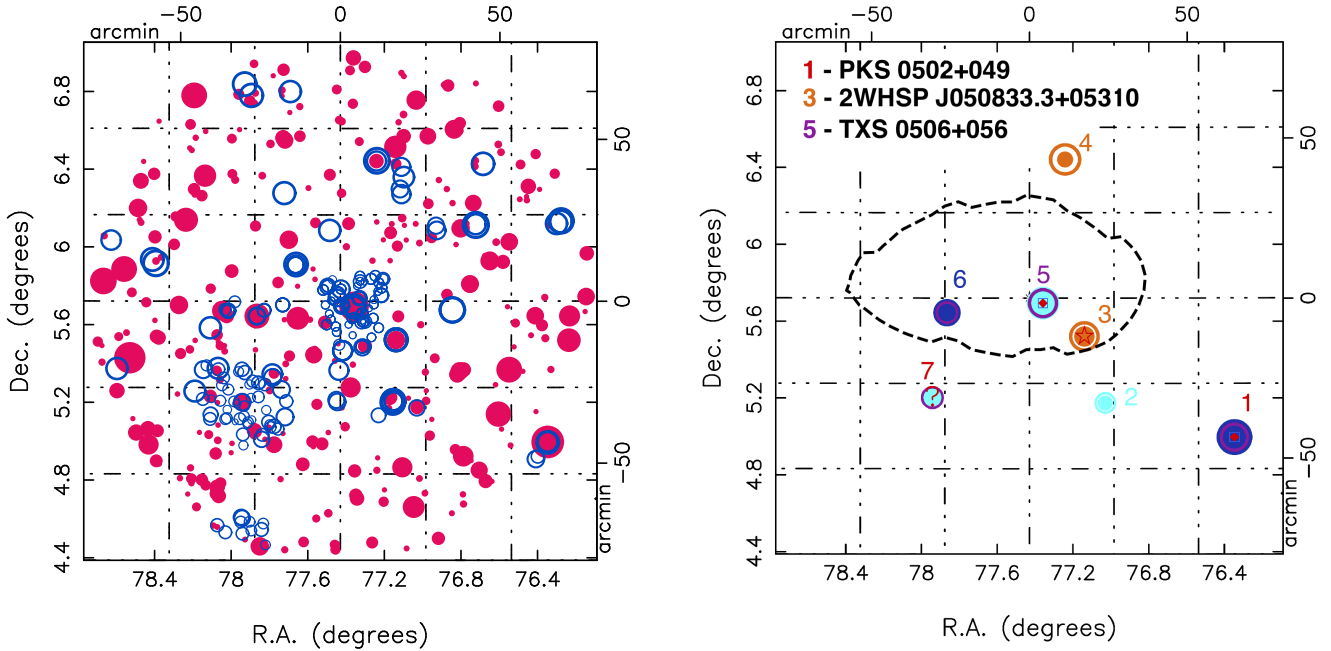


Figure 1. **Left:** Radio and X-ray sources within 80 arc-minutes of the position of IceCube-170922A. Symbol diameters are proportional to source intensity. Radio sources appear as red filled circles, X-ray sources as open blue circles. **Right:** Known and candidate blazars around IceCube-170922A as detected by a tool developed within the framework of the Open Universe initiative as described in the text. Dark blue circles represent LBL type candidates, that is sources with flux ratio in the range observed in the sample of LBL blazars of the latest edition of the BZCAT catalogue (Massaro et al. 2015), cyan symbols are for IBL type candidates, and orange symbols are for HBL candidates. Known blazars are also marked by a red diamond if they are included in the BZCAT catalogue or a star if they are part of the 2WHSP sample (see text for sources n. 2, 4, 6, and 7). The diameters of filled and open circles are proportional to radio flux density and X-ray flux, respectively. The dashed line shows the 90 per cent error contour of IceCube-170922A. The localization of the *Fermi* sources is such that the error ellipses are smaller than the size of the symbols.

2.4 γ -ray data

We used publicly available *Fermi*-LAT Pass 8 (with the P8R2.SOURCE.V6 instrument response functions) data acquired in the period from August 4, 2008 to February 10, 2018 and followed the standard procedures suggested by the *Fermi*-LAT team. Only the events with a high probability of being photons (evclass = 128, evtype = 3 [FRONT+BACK]) in the energy range of 100 MeV – 300 GeV from a region of interest (ROI) defined as a circle of radius 12° centred at the γ -ray position of TXS 0506+056 (RA, Dec = 77.364, 5.699) were analyzed. We removed a possible contamination from the Earth limb by cutting out all the events with zenith angle $> 90^\circ$ and only used the time intervals in which the data acquisition of the spacecraft was stable (DATA_QUAL > 0 && LAT_CONFIG == 1). Consistently with the event selection we used the standard Galactic (gll_iem_v06¹¹) and isotropic (iso_P8R2_SOURCE_V6_v06¹¹) models to describe the diffuse background emissions.

2.4.1 Test Statistic maps

To evaluate the presence of relevant γ -ray signatures around the arrival direction of IceCube-170922A, we built test statistics (TS) maps of the region (Mattox et al. 1996). The

test statistic for all the γ -ray analysis in this paper is defined as

$$TS = 2 \times [\ln \mathcal{L}(\text{source}) - \ln \mathcal{L}(\text{nosource})], \quad (1)$$

where $\mathcal{L}(\text{source})$ represents the nested likelihood of the data given a specific source hypothesis and $\mathcal{L}(\text{nosource})$ the likelihood of the background model. In our TS maps the signal hypothesis of a γ -ray point source is tested against a background model consisting of a diffuse Galactic and a diffuse isotropic component, as well as all the *Fermi*-LAT third source catalogue (3FGL; Acero et al. 2015) sources that lie outside the region of the TS map. While the point source is modeled using a power-law with free normalization and spectral index, the parameters of the background sources remain fixed. According to Wilks' theorem the test-statistic distributions follows a χ^2 distribution with two degrees of freedom. Hence TS values of 30 and 8 are equivalent to a 5 and 2 σ significance, respectively. We centred our 80×80 arc-minute maps at IceCube-170922A and used an equally spaced grid with 0.05° step size in right ascension and declination. For each of the grid points the *Fermi* Science Tools unbinned likelihood analysis tool *glike* was used to maximize the likelihoods in eq. (1) with respect to the free parameters. We built TS maps for different time windows and energy cuts, resolving the γ -ray activity during the periods of the neutrino detections and for energy thresholds 1 GeV, 2 GeV, and 5 GeV. Our choices are driven by the need for sufficiently high space resolution to distinguish different

¹¹ <https://fermi.gsfc.nasa.gov/ssc/data/access/lat/BackgroundModels.html>

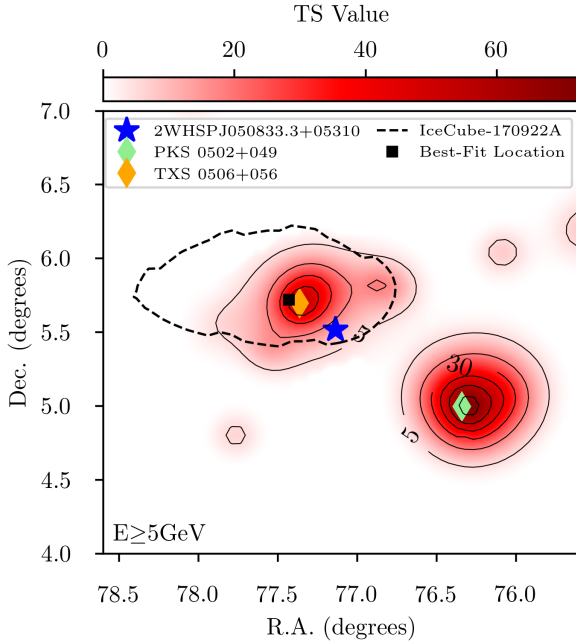


Figure 2. *Fermi* TS map based on photons with energy larger than 5 GeV between MJD 55762 and 55842 (July 20 – October 8, 2011). The dashed line shows the 90 per cent error contour of IceCube-170922A with best-fit location indicated as a black square. The solid contour lines connect points with the same TS value. Linear interpolation has been applied between the bins.

γ -ray sources (as the PSF decreases with energy) and by the fact that, given the possible neutrino production scenarios, we are mostly interested in the photons at the highest energies.

2.4.2 Light curve and photon index

γ -ray flux and photon index variations were investigated using light curves generated with a fixed time binning of 55 (28¹²) days for TXS 0506+056 (PKS 0502+049) and with an adaptive binning method with a constant relative flux uncertainty (Lott et al. 2012). In the fixed time binned light curve, photons in the 2 – 100 GeV and 0.1 – 100 GeV ranges were used for TXS 0506+056 and PKS 0502+049, respectively (see below). In the adaptive binning light curve analysis for PKS 0502+049 the fluxes are computed above an optimum energy of $E_{\min} = 214$ MeV in order to reach the required constant relative flux uncertainty of 15 per cent. For all the light curves the flux normalization and photon index of the target source are determined by applying the *gtlike* tool in each time bin. The model file, describing the ROI, contains point sources from the 3FGL catalogue within ROI+5° from the target, as well as the Galactic and isotropic γ -ray background models. It is generated using the user contributed

*make3FGLxml.py*¹³ tool. For the case of TXS 0506+056 the chosen energy threshold of 2 GeV efficiently removes any source confusion (see Fig. 4 and section 3.3), hence only this source is left free for the fit. The resulting light curve is robust against mis-modelling and strong time-variability of the other sources in the ROI. The light curve of PKS 0502+049, on the other hand, is derived by reaching lower energies, since the majority of the photons are below 1 GeV (Acero et al. 2015). In the source model both sources are fitted at the same time. The diffuse background components are fixed to their nine year value, since they are not expected to vary on the time scales of this analysis. Additionally, since we are using short integration times, we model PKS 0502+049 with a power-law.

3 PUTTING IT ALL TOGETHER

3.1 Relevant astronomical sources in the region of IceCube-170922A

We have searched for non-thermal emission in blazar-like sources in the vicinity of IceCube-170922A using a tool that is being developed in the framework of the United Nations Open Universe initiative¹⁴ using Virtual Observatory protocols. This was used to find sources in all available lists of radio and X-ray emitters. Fig. 1 (left) shows a plot of the 637 radio and X-ray sources present in those catalogues or which were detected in dedicated *Swift* observations within 80 arcminutes of the position of IceCube-170922A. Of these, only 7 emit in both bands and are all blazar-like in their X-ray-to-radio flux ratio, as determined from the BZCAT (Massaro et al. 2015) and 2WHSP (Chang et al. 2017) samples. These are shown in Fig. 1 (right).

Three known objects, i.e. TXS 0506+056 (an IBL/HBL¹⁵ at $z = 0.3365$: Paiano et al. 2018), PKS 0502+049 (also known as 5BZQ J0505+0459, an LBL/FSRQ at $z = 0.954$), and 2WHSP J050833.3+05310 (an HBL), i.e. sources no. 5, 1, and 3 respectively in Fig. 1 (right), and four additional blazar candidates are present in the area. The first two blazars are also bright γ -ray emitters (Sect. 3.2). Visual inspection of the SED of the other sources allowed us to confirm that source no. 4 is a good candidate HBL object, while source 7 is likely a cluster of galaxies (due to its extended X-ray emission), source 6 is a steep radio spectrum object, and source 2 is a nearby ($z = 0.03677$) elliptical galaxy showing low luminosity X-ray emission ($L \sim 10^{41}$ erg s⁻¹ at 1 keV) that could be due to a jet or even to non-nuclear sources.

3.2 γ -ray emission near IceCube-170922A

The γ -ray emission near IceCube-170922A is dominated at various times either by TXS 0506+056 or by PKS 0502+049 but there are also times when the two sources have roughly equal fluxes, as shown in Fig. 2. To investigate which of the

¹² This difference is due to the fact that the photon statistics for PKS 0502+049 is better than for TXS 0506+056 for the chosen energy thresholds. The bin sizes used have been chosen in order to have enough photon statistics in the majority of the bins but also to avoid any fine tuning.

¹³ <https://fermi.gsfc.nasa.gov/ssc/data/analysis/user/>

¹⁴ <http://openuniverse.asi.it>

¹⁵ A fit to the SED around the time of the neutrino alert gives $\nu_{\text{peak}}^S \sim 10^{15}$ Hz, making this an IBL/HBL source.

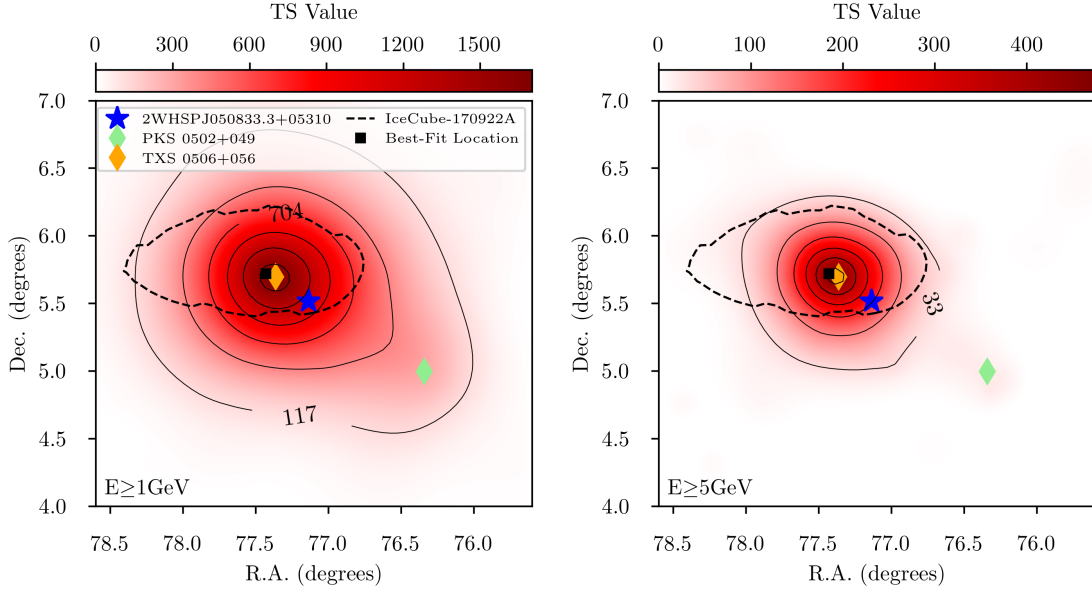


Figure 3. *Fermi* TS map based on photons with energy larger than 1 GeV (left) and 5 GeV (right) between MJD 57908 and 58018 (June 4 – September 22, 2017). In this period TXS 0506+056 is in outburst and dominates the field. See Fig. 2 for more information.

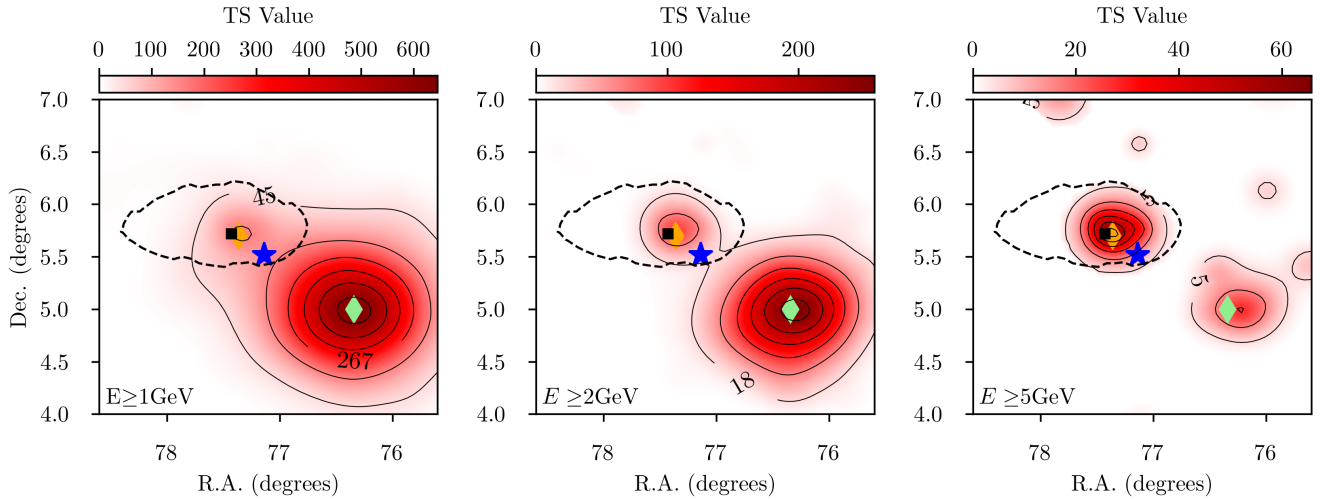


Figure 4. *Fermi* TS map based on photons with energy larger than 1, 2 and 5 GeV between MJD 56949 and 57059 (October 19, 2014 – February 6, 2015). In this period the brightest source was PKS 0502+049 at lower energies while TXS 0506+056 dominated at higher energies. See Fig. 2 for more information.

sources dominate the γ -ray emission during the IceCube-170922A event and the neutrino flare period we constructed TS maps for these two periods. We observe the following:

- (i) Fig. 3 shows the TS maps during the period contemporaneous with and before the IceCube-170922A event. From the maps it appears that TXS 0506+056 dominates the photon flux of the region at energies > 1 GeV;
- (ii) during the time of the neutrino flare, on the other hand, the situation is different, with PKS 0502+049 being the brightest source at $E > 1$ GeV and TXS 0506+056 progressively taking over above 2 and 5 GeV, as shown in Fig. 4.

We tried to unveil any evidence of γ -ray emission associated with the neighbour HBL 2WHSP J050833.3+05310, which is also within the 90 per cent error contour of IceCube-170922A, by conducting a series of eleven unbinned likelihood analyses, covering 9 years of observation with *Fermi*-LAT. We set energy cuts at $E > 1$ GeV and > 5 GeV, integrating over 400 days intervals¹⁶. We kept all 3FGL sources in the field, setting both normalizations and photon indexes as

¹⁶ Each bin has 100 days superposed to the previous/next bin, meaning we cover the following time windows: MJD 54700 to 55100, 55000 to 55400, 55300 to 55700... and so on.

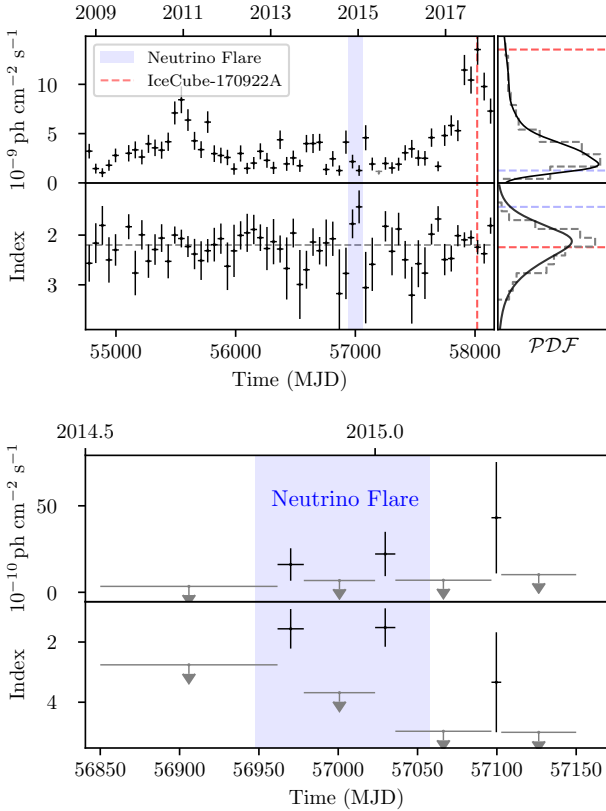


Figure 5. Top: light curve of TXS 0506+056 in 55-day bin at $E > 2$ GeV and photon index curve. All points have a TS > 9 , otherwise 95 per cent upper limits are shown. The blue band denotes the neutrino flare, while the red line indicates the IceCube-170922A event. The central horizontal line is the mean value of the spectral index. The corresponding photon flux and spectral index mean value distributions are shown as histograms (dashed grey) and kernel density estimations (solid black) in the top and bottom-right panels respectively, with the values during the neutrino flare (blue) and the IceCube-170922A event (red) indicated as dashed lines. **Bottom:** γ -ray flux and photon index of TXS 0506+056 above 10 GeV, at the time of the neutrino excess observed around MJD 57000. The photon fluxes are calculated up to 300 GeV.

free parameters. At the 2WHSP J050833.3+05310 position an additional power-law source was included in the model. The strongest signature for γ -ray emission was found between MJD 55900 to 56300 for the 1 GeV energy cut, reaching TS ~ 5 . This result was confirmed by the residual map of the region.

3.3 γ -ray light curves

As discussed in Sect. 2.4.2, we have derived the γ -ray light and spectral index curves of TXS 0506+056 and PKS 0502+049. As inferred from Fig. 4, we have evidence that PKS 0502+049 dominates the γ -ray sky at low energies during the neutrino flare, possibly contaminating TXS 0506+056 below 2 GeV. We build the light curves for TXS 0506+056 integrating photons above 2 GeV to avoid any bias from PKS 0502+049 and also study the highest en-

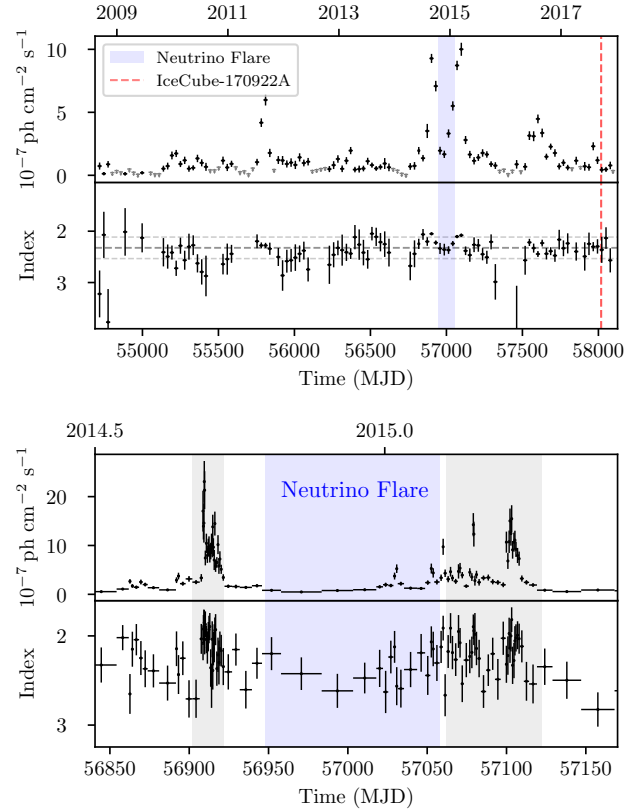


Figure 6. Top: light curve of PKS 0502+049 in 28-day bin and $E > 0.1$ GeV and photon index curve. All points have a TS > 9 , otherwise 95 per cent upper limits are shown. The blue band denotes the neutrino flare, while the red line indicates the IceCube-170922A event. The central horizontal line is the mean value of the spectral index. **Bottom:** adaptive bin light curve photon flux with $E_{\min} = 214$ MeV γ -ray light curve of PKS 0502+049 at the time of the neutrino excess observed around MJD 57000. The photon fluxes are calculated up to 300 GeV. The shaded bands at the left and right of the neutrino flare indicate the time windows where PKS 0502+049 is in a high photon flux state (see also Fig. 8).

ergies (above 10 GeV) during the specific neutrino flare period. This is the best compromise for the energy threshold. Ideally, one would like to sample as high energies as possible, to profit from the smaller *Fermi*-LAT PSF and source containment region and therefore reduce contamination from PKS 0502+049. However, the larger the energy, the smaller the photon statistics.

In contrast, we build light curves for PKS 0502+049 above 0.1 GeV with fixed time bins and above 214 MeV with the adaptive binning method to study both long and short term structures. Fig. 5 (top) shows the light curve of TXS 0506+056. The blue band denotes the neutrino flare, while the red line indicates the IceCube-170922A event. Significant flux variations are visible, as typical of blazars. The corresponding photon flux and spectral index distributions are also shown on the right. It is interesting to note that TXS 0506+056 was at its hardest in the *Fermi*-LAT band during the neutrino flare, while being relatively faint (a “low/hard” state), and at its brightest during the IceCube-

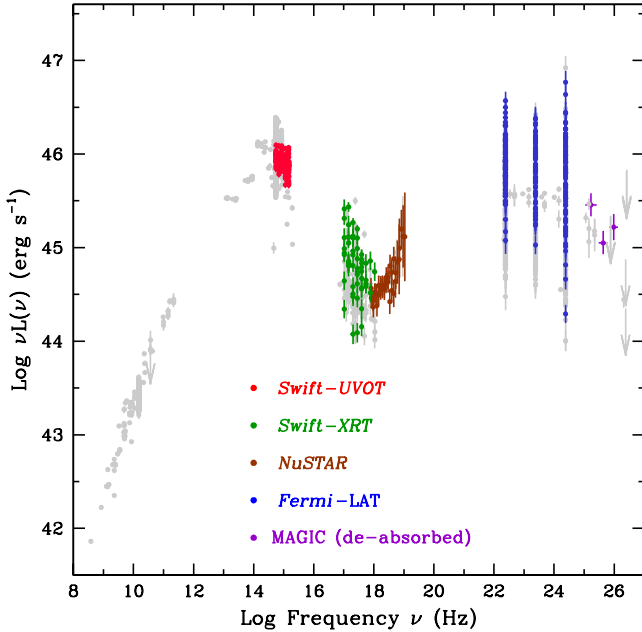


Figure 7. The SED of TXS 0506+056 assembled using all available public data. The blue measurements in the γ -ray band show the variability at 0.1, 1, and 10 GeV using *Fermi*-LAT data collected between January 1 and December 31, 2017 (see Fig. 10 for the 1 and 10 GeV light curves). Green and brown points at X-ray frequencies are from our analysis of *Swift* and *NuSTAR* data respectively. MAGIC data (*IceCube Collaboration 2018a*) are shown as purple crosses and were de-absorbed to correct for the extragalactic background light following *Domínguez et al. (2011)*. Red points at optical and UV frequencies are from *Swift*-UVOT. The other non-simultaneous multi-frequency measurements are from catalogues and online archives (grey points).

170922A event, while being softer (a “high/soft” state). Note that, based on the overall distributions, a spectral index as hard as observed during the neutrino flare is expected with a probability of only ~ 2 per cent, while a flux as high as that during the IceCube-170922A event has a probability of only ~ 1 per cent to be detected. The average photon index during the entire duration of the neutrino flare for $E > 2$ GeV is 1.62 ± 0.20 .

Since we want to concentrate on the highest energy photons we zoom in on the period around the neutrino flare to investigate in more detail the source variability looking for the most extreme emission using only events above 10 GeV. The period from MJD 56850 to MJD 56750 was then divided into half- and one-day bins and an unbinned maximum likelihood analysis was performed. Next, the nearby bins with $TS > 0$ were merged and new light curves were calculated. In order to improve the statistics, the length of the time periods with $TS > 0$ was then progressively increased by adding 1-hour intervals. As a result, we find two periods with significant emission above 10 GeV (Fig. 5, bottom): MJD 56961.75 – 56978.29 ($TS = 30.5$), with the highest energy photon at

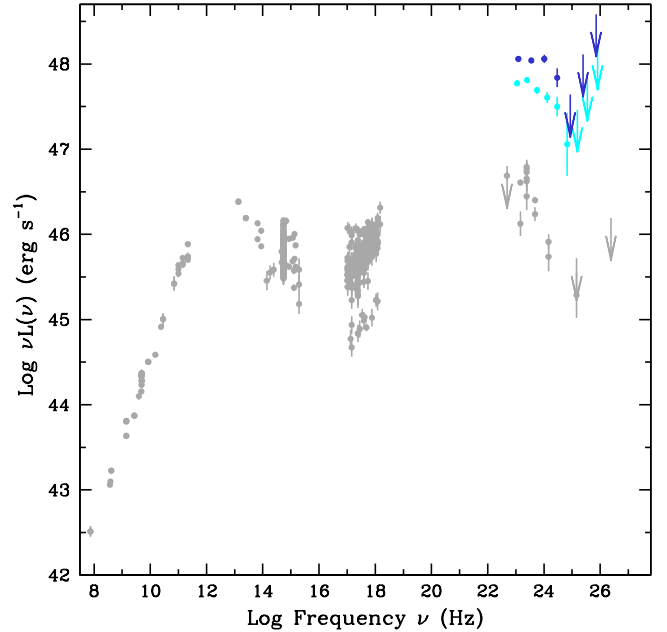


Figure 8. The SED of PKS 0502+049. The γ -ray spectra during the two flaring periods (see Fig. 6, bottom) are shown as blue (MJD 56902 – 56922) and cyan (MJD 57062 – 57122) points. All other multi-frequency data are non-simultaneous archival data.

53.3 GeV, and MJD 57023.25 – 57036.0 ($TS = 33.6$), with the highest energy photon at 52.6 GeV¹⁷.

Fig. 6 shows the light curve of PKS 0502+049. The blue band denotes the neutrino flare, while the red line indicates the IceCube-170922A event. Significant flux variations are also visible in this case in particular in the periods right before and after the neutrino flare but the overlap with the neutrino flare is minimal even taking into account the uncertainties on its duration as clearly visible in the adaptive bin zoom-in (see Fig. 6 bottom; the neutrino flare covers 110^{+35}_{-24} days and we did not consider small γ -ray fluctuations over much shorter time scales). PKS 0502+049 presents no particular states in photon flux and/or spectral index during IceCube-170922A and the neutrino flare period.

3.4 Spectral energy distributions

Fig. 7 shows the SED of TXS 0506+056. The *NuSTAR* data show a hardening at $\sim 10^{18}$ Hz ($\sim 4 - 5$ keV) most likely due to the onset of the inverse Compton component (e.g. *Padovani et al. 2017*). Fig. 8 shows the SED of PKS 0502+049. Two points can be made: (1) during flares PKS 0502+049 is a brighter γ -ray source than TXS 0506+056; (2) the SED of PKS 0502+049 cuts off at $E \approx 10$ GeV, while that of TXS 0506+056 reaches $E \gtrsim 100$ GeV (compatibly with the likely extragalactic background light absorption at its redshift: *Paiano et al. 2018*).

To study the time evolution of the SED of

¹⁷ Based on the *gtsrcprob* tool both of these photons have a > 99 per cent probability of being related to TXS 0506+056

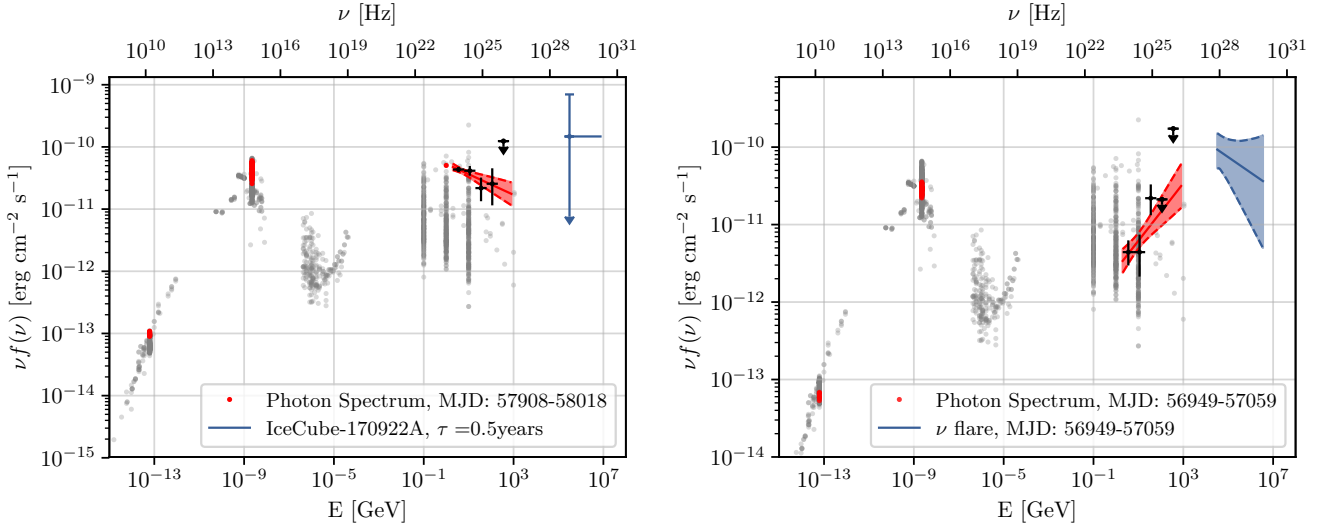


Figure 9. The hybrid photon – neutrino SED of TXS 0506+056. The red points (OVRO at 15 GHz and ASAS V_{mag}) are simultaneous with neutrinos, grey ones refer to historical data, while the black ones are *Fermi* data. The red bands for the γ -ray flux show the 1σ error bounds on the best fit, while upper limits are given at 95 per cent C.L.. *Fermi* data points were de-absorbed to correct for the extragalactic background light following Domínguez et al. (2011). **Left:** the MJD 57908 – 58018 period (June 4 – September 22, 2017). The neutrino flux has been derived by IceCube Collaboration (2018a) over the 200 TeV – 7.5 PeV range (see text for more details); we give here the all-flavour flux. The vertical upper limit is drawn at the most probable neutrino energy. The average *Fermi*-LAT photon index for $E > 2$ GeV is 2.16 ± 0.10 . **Right:** the MJD 56949 – 57059 period (October 19, 2014 – February 6, 2015). The neutrino flux has been derived by IceCube Collaboration (2018b) over the 32 TeV – 3.6 PeV range; the error is the combined error on the spectral index and the normalization. The average *Fermi*-LAT photon index for $E > 2$ GeV is 1.62 ± 0.20 .

TXS 0506+056 we have built an animation of nearly simultaneous data, which include 15 GHz monitoring data from OVRO, the ASAS V_{mag} light curve (Kochanek et al. 2017), the optical/UV data of the *Swift*-UVOT (Roming et al. 2005) analyzed with the SSDC online tool, and the X-ray and γ -ray data described in sect 2.3 and 2.4. The animation is available here: <https://youtu.be/lFBciGIT0mE>.

3.4.1 The hybrid SED of TXS 0506+056

Fig. 9 shows the hybrid photon – neutrino SED of TXS 0506+056 for the period around the IceCube-170922A event (left) and the neutrino flare (right), based on the concept introduced by Padovani & Resconi (2014). The red points are the electromagnetic emission simultaneous with the neutrinos. The detection of high-energy neutrinos above ~ 30 TeV implies the existence of protons up to at least $3 \times 10^{14} - 3 \times 10^{15}$ eV, which then collide with other protons (pp collisions) or photons ($p\gamma$ collisions). High-energy γ -rays with energy and flux about a factor two higher than the neutrinos at the source are then expected as secondary products in both cases (Kelner, Aharonian, & Bugayov 2006; Kelner & Aharonian 2008). Indeed, in both cases the (linearly extrapolated) γ -ray and neutrino fluxes are comparable, consistently with the hypothesis that they are produced by the same physical process. This is especially true for the neutrino flare, when the neutrino flux has a relatively small uncertainty being derived from ~ 13 events within a well-defined period of 110^{+35}_{-24} days (IceCube Collaboration 2018b).

This is different for the IceCube-170922A event, given the large uncertainty on the neutrino flux since we are dealing with a single event over an ill-defined period of time. To

estimate the neutrino flux from one neutrino event IceCube Collaboration (2018a) had to assume a spectral emission shape, an emission time τ , and an energy emission range. The corresponding mean number of ν_μ events N expected in IceCube is

$$N = \tau \int_{E_{\min}}^{E_{\max}} A_{\text{eff}}(E, \theta) \cdot \frac{1}{3} \frac{d\phi}{dE} dE, \quad (2)$$

where A_{eff} is the effective area of the IceCube detector and $\frac{1}{3}$ is the flavour ratio assumed. For a source described by a single power-law distribution the flux producing one neutrino event is

$$\phi_0 = \frac{3 \cdot N}{\tau \int_{E_{\min}}^{E_{\max}} A_{\text{eff}}(E, \theta) E^{-\gamma} dE}, \quad (3)$$

where $N = 1$ and τ is taken as 0.5 years (of the same order as the duration of the γ -ray flare). Interpreting the observation of one IceCube alert event as an upward Poissonian fluctuation, then the flux value calculated can be understood as an upper limit on the neutrino flux (see also IceCube Collaboration 2018a).

4 RESULTS

Following up the IceCube-170922A event observed in coincidence with a γ -ray flare of TXS 0506+056 (IceCube Collaboration 2018a), the IceCube collaboration has also detected a neutrino flare in late 2014 – early 2015 from the same direction (IceCube Collaboration 2018b). Given the complexity

of the γ -ray sky in this area, both spatially and temporally, we have carefully dissected the region and found the following:

(i) out of the 637 radio and X-ray sources within 80 arc-minutes of the IceCube-170922A event position, only 7 are both radio and X-ray emitters and therefore likely non-thermal sources. As it turns out, the X-ray-to-radio flux ratios of these 7 sources are blazar-like;

(ii) out of these 7 sources, 4 are blazars, two of which are very bright γ -ray sources, namely TXS 0506+056 and PKS 0502+049, competing for dominance;

(iii) while TXS 0506+056 dominates in all γ -ray bands during the IceCube-170922A event, the situation is more complex during the neutrino flare, as PKS 0502+049 dominates up to $E \sim 1 - 2$ GeV but TXS 0506+056 takes over at $E \gtrsim 2 - 5$ GeV. The γ -ray spectrum of PKS 0502+049, in fact, cuts off at high energy even during flares, a behaviour typical of LBL blazars;

(iv) PKS 0502+049 is flaring right before and right after the neutrino flare (but not in coincidence with it) while TXS 0506+056 was at its hardest in that time period but in a relatively faint state, suggesting a shift to high energies of the γ -ray SED;

(v) the hybrid γ -ray – neutrino SED of TXS 0506+056 during the neutrino flare is as expected for lepto-hadronic models since the photon and neutrino fluxes are at the same level (Petropoulou et al. 2015). We note that the hybrid SEDs of Padovani & Resconi (2014) and Padovani et al. (2016) were based on *one* shower-like IceCube event, which could in principle have been emitted over the full IceCube detection live time, and were therefore affected by a very large uncertainty. In the case of the neutrino flare, instead, a *sizable* (~ 13) number of neutrinos has been detected within a well-defined time window and good spatial resolution.

In short, all spatial, timing, and energetic multi-messenger diagnostics point to TXS 0506+056 as the first identified non-stellar neutrino (and therefore cosmic ray) source.

5 DISCUSSION

5.1 Source properties

We now explore in more detail the properties of TXS 0506+056. First, we note that this source is a very strong γ -ray source, having an average flux of 7.1×10^{-8} ph cm $^{-2}$ s $^{-1}$ above 100 MeV, which puts it among the top 4 per cent of the *Fermi* 3LAC catalogue (Ackermann et al. 2015). Moreover, it also belongs to the 2FHL sample (Ackermann et al. 2016), which includes all sources detected above 50 GeV by *Fermi*-LAT in 80 months of data. TXS 0506+056 also has a large radio flux density ~ 1 Jy at 6 cm (Gregory & Condon 1991), and ~ 537 mJy at 20 cm, which makes it one of the brightest radio sources (in the top 0.3 per cent) of the NRAO VLA Sky Survey, which covers 82 per cent of the sky (Condon et al. 1998). Fig. 7 shows the overall SED of the source in luminosity, based on the redshift of 0.3365 recently reported by Paiano et al. (2018).

The peak luminosities of $\sim 2 \times 10^{46}$ erg s $^{-1}$ in the synchrotron peak, and almost 10^{47} erg s $^{-1}$ at 10 GeV, place this

object among the most powerful BL Lacs known, particularly in the high-energy/very high-energy γ -ray band. For comparison, the corresponding maximum luminosities ever observed in MKN 421 (and PKS 2155–304) are $\sim 4 \times 10^{45}$ ($\sim 2 \times 10^{46}$) and $\sim 1.5 \times 10^{45}$ (10^{46}) erg s $^{-1}$, a factor of ~ 5 (1) and ~ 50 (10) lower than TXS 0506+056 (Giommi et al., in preparation). What seems to be peculiar in this source is the very large luminosity at ~ 10 GeV compared to other similar sources. From the overall SED point of view TXS 0506+056 shows a variability range in the γ -ray band (almost a factor 1,000 at 10 GeV: see Fig. 7) much larger than that observed at the peak of the synchrotron emission. Even during the large γ -ray flaring event observed close to the detection of IceCube-170922A the peak of the synchrotron emission (located in the UV band) did not vary by more than a factor of 2, nor did the X-ray flux, at the tail of the synchrotron peak, change by a large factor. This behaviour is consistent with an excess of hard γ -ray radiation possibly associated with hadronic processes.

We now possess all the elements to calculate reliably the luminosity of a high-energy neutrino source. Using the fluence, spectral index, and energy range given in Sect. 2.1.2 and IceCube Collaboration (2018b) we do the following: 1. derive an integrated ν_μ flux of 1.2×10^{-10} erg cm $^{-2}$ s $^{-1}$ from the fluence by integrating over the 2σ range around the central value of the time period; 2. estimate L_{ν_μ} ; 3. derive a neutrino luminosity all-flavour (assuming $\nu_e : \nu_\mu : \nu_\tau = 1 : 1 : 1$) by multiplying by 3 the ν_μ power. The result is $L_\nu = 3 \times L_{\nu_\mu} \sim 3 \times 4.5 \times 10^{46}$ erg s $^{-1} \sim 1.4^{+0.6}_{-0.5} \times 10^{47}$ erg s $^{-1}$ between 32 TeV and 3.6 PeV. (This luminosity is fully consistent with the one derived by IceCube Collaboration (2018b) of $1.2^{+0.6}_{-0.4} \times 10^{47}$ erg s $^{-1}$ based on a flare duration of 158 days derived from the box time-window result.)

This can be compared to the *simultaneous* γ -ray luminosity L_γ (2 GeV – 1 TeV)¹⁸ $\sim 3 \times 10^{46}$ erg s $^{-1}$ [or L_γ (2 GeV – 100 GeV) $\sim 10^{46}$ erg s $^{-1}$].

5.2 Physical implications

Our results have several physical implications. Namely:

(i) with neutrinos we are exploring an energy range which is inaccessible with photons at this redshift. Therefore, the first evidence for neutrino emission from the direction of TXS 0506+056 opens a new window on blazar physics;

(ii) the derived L_ν during the neutrino flare is quite large and even larger than L_γ (2 GeV – 1 TeV), which might imply that a sizeable fraction of the neutrino-related γ -rays have energies above the *Fermi*-LAT energy band, as expected in the case of *py* collisions (Sect. 3.4.1);

(iii) the ratio between the two SED humps (high-energy to low-energy, usually known as Compton dominance [CD]: e.g. Giommi et al. 2012b) for TXS 0506+056 is > 1 , while typical HBL have CD ~ 0.1 . This could be due to the electromagnetic emission coming from different blobs e.g. one dominant at optical frequencies and the other dominant at high-energy γ -rays, or to the presence of an additional hadronic component in the γ -ray band;

¹⁸ This is based on the *Fermi*-LAT best fit extrapolated to 1 TeV.

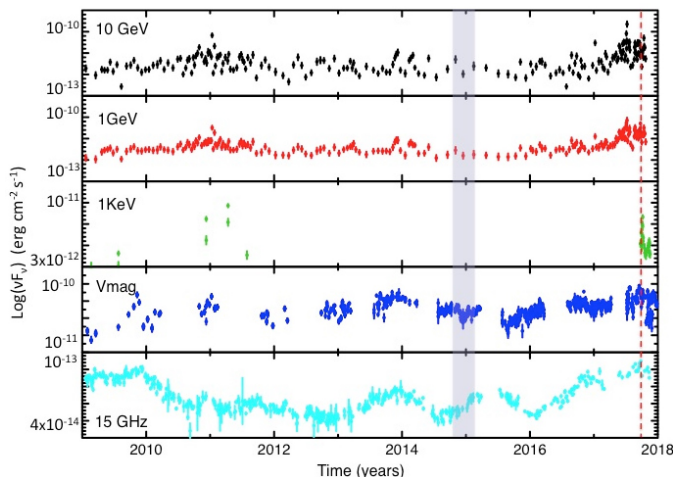


Figure 10. The radio (15 GHz), optical (V_{mag}), X-ray and γ -ray light curves of TXS 0506+056. The radio data have been taken from the OVRO database, the visual magnitude data are from the Catalina Real Time Transient Survey (CRTS) and from the All Sky Automatic Survey ASAS (Kochanek et al. 2017). The γ -ray light curves have been produced using *Fermi*-LAT data with the adaptive-bin method (Lott et al. 2012). The blue band denotes the neutrino flare, while the red line indicates the IceCube-170922A event.

(iv) a discrete cross-correlation analysis using the z-transformed discrete correlation function (ZDCF; Alexander 1997) among the radio (15 GHz), optical, X-ray and γ -ray light curves of TXS 0506+056, was built with the data described in the previous paragraphs (Fig. 10). The ZDCF shows a strong correlation ($\sim 10\sigma$) with a time lag of ≈ 4 months between the radio and optical emission (with the optical band leading) but no correlation between optical/X-ray/radio and γ -ray bands. This is at variance with typical single-zone leptonic (synchrotron self-Compton or external Compton) models where all energy bands are expected to be well correlated;

(v) the SED of at least one blazar now *has* to be modeled within a lepto-hadronic scenario (e.g. Petropoulou et al. 2015). This is far from trivial and goes well beyond the scope of this paper;

(vi) the neutrino sky has been populated so far by only two sources: the Sun (e.g. BOREXINO Collaboration et al. 2014) and SN 1987A (Hirata et al. 1987; Bionta et al. 1987; Alekseev et al. 1987). TXS 0506+056 is now a third plausible candidate, whose neutrino energies are, however, more than six orders of magnitude larger than those of the two stellar sources.

5.3 Future searches

Our results suggest two periods of neutrino emission for TXS 0506+056, which appear to be in connection with two very different γ -ray states, namely one high/soft, connected to the IceCube-170922A event, and another one low/hard, related to the neutrino flare. This implies that the search for multi-messenger sources needs to be carried out not only for flaring γ -ray sources but also for relatively hard emit-

ters. These criteria can also be used by neutrino telescopes to look for other neutrino sources.

Why is this the only strong IceCube neutrino source candidate? What makes it special? We believe this is due to a series of factors. First, as discussed in Sect. 5.1, TXS 0506+056 is a very strong γ -ray and radio source. Moreover, its declination and energy range happened to be in the regions of parameter space where IceCube reaches maximum sensitivity and the duration of the flare was also long enough for IceCube to (marginally) detect it (see also IceCube Collaboration 2018b).

Future searches for cosmic neutrino sources should emphasize: (1) extreme blazars of the BL Lac type, as hinted at by Padovani et al. (2016); (2) high/soft – low/hard γ -ray states; (3) regions of parameter space where the neutrino detectors are most sensitive.

6 CONCLUSIONS

The IceCube-170922A event and the neutrino flare at the end of 2014 have been linked to the same source, TXS 0506+056, a blazar of the BL Lac type at $z = 0.3365$. This is the most plausible association so far between IceCube neutrinos and an extragalactic object. The area near TXS 0506+056 is quite complex due to the presence of several non-thermal sources, which in principle could all contribute to the overall γ -ray flux. We have therefore carefully dissected this region using a multi-messenger approach, obtaining the following results:

(i) TXS 0506+056 was the brightest *Fermi* source in the region of interest at energies above 1 GeV during the IceCube-170922A event but only above 2–5 GeV during the neutrino flare. PKS 0502+049, a nearby blazar of the FSRQ type offset by $\sim 1.2^\circ$, dominated the γ -ray region at lower energies in the latter period.

(ii) We have observed two periods of significant neutrino emission consistent with the position of TXS 0506+056 in connection with two very different γ -ray states, namely one, high/soft, connected to the IceCube-170922A event, and another one, low/hard, related to the neutrino flare. PKS 0502+049 was also flaring right before and right after the neutrino flare but not in coincidence with it.

(iii) We have built the hybrid photon – neutrino SED of TXS 0506+056 during the neutrino flare and have reliably estimated the power of a high-energy neutrino source. This is $\sim 1.4 \times 10^{47} \text{ erg s}^{-1}$ between 32 TeV and 3.6 PeV (all-flavour), even larger than the *simultaneous* L_γ (2 GeV – 1 TeV) $\sim 3 \times 10^{46} \text{ erg s}^{-1}$.

(iv) Both the lack of a correlation between the γ -ray and radio/optical flux and the SED shape of TXS 0506+056, which is unusual in terms of its Compton dominance, appear not to be consistent with simple leptonic models.

(v) All of the above is fully consistent with the hypothesis that TXS 0506+056 has undergone a hadronic flare during the neutrino detections.

In short, all spatial, timing, and energetic multi-messenger diagnostics point to TXS 0506+056 as the only counterpart of all the neutrinos observed in the vicinity of IceCube-170922A and therefore the first non-stellar neutrino (and hence cosmic ray) source. The emergent picture is that

extreme blazars, i.e., strong, very high energy γ -ray sources with the peak of the synchrotron emission $> 10^{14} - 10^{15}$ Hz (Padovani et al. 2016), are the first class of sources with evident contribution to the IceCube diffuse signal (IceCube Collaboration 2017a,b).

Future searches for cosmic neutrino sources, concentrated on similar classes of sources, using additional high-energy track-like events, and based on detailed multi-messenger analysis, will likely provide further associations.

ACKNOWLEDGMENTS

We acknowledge the use of data and software facilities from the SSDC, managed by the Italian Space Agency, and preliminary versions of other software tools currently being developed within the United Nations “Open Universe” initiative. PG acknowledges the support of the Technische Universität München - Institute for Advanced Studies, funded by the German Excellence Initiative (and the European Union Seventh Framework Programme under grant agreement n. 291763). BA is supported by the São Paulo Research Foundation (FAPESP) with grant n. 2017/00517-4. This work is supported by the Deutsche Forschungsgemeinschaft through grant SFB 1258 “Neutrinos and Dark Matter in Astro- and Particle Physics”. We thank the IceCube collaboration for granting us access to information prior to publication, through a Memorandum of Understanding. We thank Markus Ahlers, Dave Seckel, and Justin Vandenbroucke for fruitful discussions and the referee, Dr. Ralph Wijers, and the scientific editor for useful and swift comments. The *Fermi*-LAT Collaboration acknowledges generous ongoing support from a number of agencies and institutes that have supported both the development and the operation of the LAT as well as scientific data analysis. These include the National Aeronautics and Space Administration and the Department of Energy in the United States, the Commissariat à l’Energie Atomique and the Centre National de la Recherche Scientifique / Institut National de Physique Nucléaire et de Physique des Particules in France, the Agenzia Spaziale Italiana and the Istituto Nazionale di Fisica Nucleare in Italy, the Ministry of Education, Culture, Sports, Science and Technology (MEXT), High Energy Accelerator Research Organization (KEK) and Japan Aerospace Exploration Agency (JAXA) in Japan, and the K. A. Wallenberg Foundation, the Swedish Research Council and the Swedish National Space Board in Sweden. Additional support for science analysis during the operations phase is gratefully acknowledged from the Istituto Nazionale di Astrofisica in Italy and the Centre National d’Études Spatiales in France.

REFERENCES

- Aartsen M. G., et al., 2013, *Phys. Rev. Lett.*, 111, 021103
Aartsen M. G., et al., 2015, *Phys. Rev. Lett.*, 115, 081102
Aartsen M. G., et al., 2016, *ApJ*, 833, 3
Aartsen M. G., et al., 2017, *ApJ*, 835, 45
Acero, F., Ackermann, M., Ajello, M., et al. 2015, *ApJS*, 218, 23
Ackermann M., et al., 2011, *ApJ*, 743, 171
Ackermann M., et al., 2015, *ApJ*, 810, 14
Ackermann M., et al., 2016, *ApJS*, 222, 5
Ahlers M., Halzen F., 2015, *Rep. Prog. Phys.*, 78, 126901
Alexander T., 1997, *Astrophysics and Space Science Library* Vol. 218, 163
Alekseev E. N., Alekseeva L. N., Volchenko V. I., Krivosheina I. V., 1987, *PZETF*, 45, 461
Atwood W. B., et al., 2009, *ApJ*, 697, 1071
Bionta R. M., et al., 1987, *PhRvL*, 58, 1494
BOREXINO Collaboration, et al., 2014, *Nature*, 512, 383
Burrows D., et al. 2005, *Space Science Rev.* 120, 165
Chang Y.L., Arsoli B., Giommi P. & Padovani P., 2017, *A&A*, 598, 17
Condon J. J., Cotton W. D., Greisen E. W., Yin Q. F., Perley R. A., Taylor G. B., Broderick J. J., 1998, *AJ*, 115, 1693
Domínguez A., et al., 2011, *MNRAS*, 410, 2556
Fiore F., et al., 2017, *A&A*, 601, A143
Gehrels N. et al. 2004, *ApJ*, 611, 1005
Ghisellini G., Righi C., Costamante L., Tavecchio F., 2017, *MNRAS*, 469, 255
Giommi P., Padovani P., Polenta G., Turriziani S., D’Elia V., Piranomonte S., 2012a, *MNRAS*, 420, 2899
Giommi P. et al., 2012b, *A&A* 541, 160
Giommi P., 2015, *JHEAp*, 7, 173
Giommi P., Padovani P. & Polenta G., 2013, *MNRAS*, 431, 1914.
Giommi P., Padovani P., 2015, *MNRAS*, 450, 2404
Gregory P. C., Condon J. J., 1991, *ApJS*, 75, 1011
Halzen F., Zas E., 1997, *ApJ*, 488, 669
Harrison F., et al., 2013 *ApJ*, 770, 103
Hirata K., et al., 1987, *PhRvL*, 58, 1490
IceCube Collaboration, 2013, *Science*, 342, 1242856
IceCube Collaboration, 2014, *Phys. Rev. Lett.*, 113, 101101
IceCube Collaboration, 2015a, Contributions to the 34th International Cosmic Ray Conference (ICRC 2015), p. 45 (arXiv:1510.05223)
IceCube Collaboration, 2015b, Contributions to the 34th International Cosmic Ray Conference (ICRC 2015), p. 37 (arXiv:1510.05223)
IceCube Collaboration, 2017a, Contributions to the 35th International Cosmic Ray Conference (ICRC 2017), p. 30 (arXiv:1710.01191)
IceCube Collaboration, 2017b, Contributions to the 35th International Cosmic Ray Conference (ICRC 2017), p. 54 (arXiv:1710.01191)
IceCube Collaboration, 2017c, Contributions to the 35th International Cosmic Ray Conference (ICRC 2017), p. 31 (arXiv:1710.01179)
IceCube Collaboration, 2018a, *Science*, submitted
IceCube Collaboration, 2018b, *Science*, submitted
Keivani A., et al., 2017, *GCN*, 21930, 1
Kelner S. R., Aharonian F. A., Bugayov V. V., 2006, *Phys. Rev. D*, 74, 034018
Kelner S. R., Aharonian F. A., 2008, *Phys. Rev. D*, 78, 034013
Kochanek, C. S. et al. 2017, *PASP*, 129, 4502
Kopper C., Blaufuss E., 2017, *GCN*, 21916, 1
Lott B., Escande L., Larsson S., Ballet J., 2012, *A&A*, 544, A6
Lucarelli F., et al., 2017a, *ApJ*, 846, 121
Lucarelli F., et al., 2017b, *ATel*, 10801
Mannheim K., 1995, *Astroparticle Physics*, 3, 295
Massaro E., et al. 2015, *Ap&SS* 357, 75
Mattox, J. R., Bertsch, D. L., Chiang, J., et al. 1996, *ApJ*, 461, 396
Mücke A. et al., 2003, *Astroparticle Physics*, 18, 593
Padovani P., Giommi P., 1995, *ApJ*, 444, 567
Padovani P., Resconi E., 2014, *MNRAS*, 443, 474 (PR14)
Padovani P., Giommi P., 2015, *MNRAS*, 446, L41
Padovani P., Resconi E., Giommi P., Arsoli B., Chang Y. L., 2016, *MNRAS*, 457, 3582
Padovani P., et al., 2017, *A&ARv*, 25, 2
Paiano S., Falomo R., Treves A., Scarpa R., 2018, *ApJ*, 854, L32
Palladino A., Vissani F., 2017, *A&A*, 604, A18

- Petropoulou M., Dimitrakoudis S., Padovani P., Mastichiadis A., Resconi E., 2015, MNRAS, 448, 2412
Resconi E., Coenders S., Padovani P., Giommi P., Caccianiga L., 2017, MNRAS, 468, 597
Roming P.W., 2005, Space Sci. Rev., 120, 95
Tavecchio F., Ghisellini G., 2015, MNRAS, 451, 1502
Taylor M. B. 2005, Astronomical Data Analysis Software and Systems XIV, 347, 29
Urry C. M., Padovani P., 1995, PASP, 107, 803

This paper has been typeset from a \TeX / \LaTeX file prepared by the author.